Journal of Structural Geology 33 (2011) 918–927

Contents lists available at ScienceDirect

Journal of Structural Geology

journal homepage: www.elsevier.com/locate/jsg

Fractal vein distributions within a fault-fracture mesh in an exhumed accretionary mélange, Chrystalls Beach Complex, New Zealand

Åke Fagereng [a,b,*]

[a] Department of Geology, University of Otago, PO Box 56, Dunedin 9054, New Zealand
[b] Department of Geological Sciences, University of Cape Town, Private Bag X3, Rondebosch 7701, South Africa

ARTICLE INFO

Article history:
Received 9 December 2010
Received in revised form
23 February 2011
Accepted 28 February 2011
Available online 5 March 2011

Keywords:
Hydrothermal veins
Mélange
Fracture distribution
Fault-fracture mesh
Otago Schist

ABSTRACT

A well developed fault-fracture mesh is observed in the Chrystalls Beach Complex, an accretionary mélange within the Otago Schist on the South Island of New Zealand. In this study, an analysis of vein thicknesses and clustering of veins is presented. Both shear and extension veins have a power-law thickness distribution. Measures of vein spacing best fit a power-law distribution, but a small data set limits this interpretation to a small fractal range. Vein clustering varies from random to moderately clustered between outcrops, and is the greatest where a large proportion of relatively competent blocks occurs within the mélange. Fractures are distributed within the mélange matrix, and this localized deformation requires heterogeneity in rheology and/or fluid pressure distribution, whereas pervasive, distributed deformation occurs in relatively homogeneous rock. The overall trend of this deformation being mainly accommodated by thin veins required that new fractures formed preferentially over refracturing existing veins, which highlights the distributed nature of deformation within a fault-fracture mesh. The predominance of new fractures may result from vein material being stronger than the cleaved wall rock, such that wall rock failure occurred instead of reopening of pre-existing shear and extension veins.

1. Introduction

Hydrothermal veins are generally interpreted to form by brittle fracture followed by fluid infiltration and subsequent mineral precipitation (e.g. Ramsay, 1980; Cox and Etheridge, 1983; Ramsay and Huber, 1987; Sibson, 1987; Urai et al., 1991; Robert et al., 1995; Passchier and Trouw, 2005; Barker et al., 2006; Fagereng et al., 2010). The distribution of veins within a deformed rock mass therefore reflects both the local stress field at the time of fracturing and the development of structural permeability and consequent hydrological properties of the rocks. Statistical analyses of vein systems, generally characterizing vein thickness and vein distribution in 1-d, 2-d or 3-d, have therefore been applied by several authors to address vein forming mechanisms and localization of fracturing and fluid percolation (e.g. Velde et al., 1991; Sanderson et al., 1994, 2008; Clark et al., 1995; Fisher et al., 1995; Gillespie et al., 1999; Roberts et al., 1999; Simpson, 2000; André-Mayer and Sausse, 2007; Ortega et al., 2010). These previous studies have, however, focused on the distribution of opening mode fractures. Permeability is, on the other hand, in some instances enhanced by the generation of a fault-fracture mesh (Hill, 1977; Sibson, 1996). In a fault-fracture mesh, conditions governing the location of both extension fractures and dilational shears (Fagereng et al., 2010) are critically important to the development of permeability. An understanding of the mechanism of mesh generation may therefore be gained by a statistical study of the distribution of shear and extension veins, in a location favoring the development of an interconnected fault-fracture network.

Microstructures reflecting episodic fracture are evident in 'crack-seal' shear and extension veins within a fault-fracture mesh in the Chrystalls Beach Complex, New Zealand (Nelson, 1982; Fagereng et al., 2010). The distribution of these veins should give clues to the processes governing their formation. Frequency-size distributions of vein thicknesses should reflect differing nucleation and growth rates (Velde et al., 1991; Clark et al., 1995) and the degree of fracture connectivity and localization (Sanderson et al., 1994, 2008; Roberts et al., 1999; Sanderson and Zhang, 2004). Vein spacing size-frequency distributions can be used to infer the processes governing the position of fractures becoming veins (McCaffrey et al., 1993; Fisher et al., 1995; Gillespie et al., 1999; Simpson, 2000), and if the vein spacing is non-uniform, the clustering of veins quantifies the degree of pervasive versus localized

* Department of Geological Sciences, University of Cape Town, Private Bag X3, Rondebosch 7701, South Africa. Tel.: +27 21 650 2926.
E-mail address: ake.fagereng@uct.ac.za.

0191-8141/$ – see front matter © 2011 Elsevier Ltd. All rights reserved.
doi:10.1016/j.jsg.2011.02.009

fracturing (Manning, 1994). This contribution presents a data set for the thickness and spacing distributions of shear and extension veins in the Chrystalls Beach Complex. The data are used to address the processes during fracture network formation, with focus on the development of a distributed fracture system versus localization in a few existing fractures.

2. Geological setting

2.1. The Chrystalls Beach Complex

The Chrystalls Beach Complex is exposed along the southeast Otago coastline, about 60 km south of the city of Dunedin (Fig. 1). The complex has been interpreted as an accretionary mélange (Nelson, 1982; Hada et al., 2001), deformed during Triassic-Jurassic subduction along the Gondwana continental margin (Hada et al., 2001). Although interpreted as part of the Otago Schist accretion-collision assemblage (Mortimer, 1993), the stratigraphic position of the complex within this metamorphic belt is uncertain (Coombs et al., 2000). However, formation at the base of the accretionary prism has been suggested (Fagereng and Cooper, 2010a). In the Otago Schist, regional metamorphic gradients result from burial and later uplift of the rocks in the prism (e.g. Mortimer, 2000). The highest metamorphic grades are recorded along the Otago Antiform, along the center of the Otago Schist, and decrease toward the flanks, a pattern attributed to greater exhumation along the Otago Antiform (Mortimer, 1993, 2003). The Chrystalls Beach Complex experienced pumpellyite-actinolite facies metamorphism, with estimated peak, syn-tectonic, pressure-temperature conditions of 550 MPa and 300 °C (Fagereng and Cooper, 2010b).

The rock assemblage in the Chrystalls Beach Complex comprises asymmetric lenses ('phacoids') of sandstone, chert and minor basalt enclosed within a relatively incompetent, cleaved mudstone matrix (Figs. 2 and 3). This assemblage was intensely sheared in a mixed continuous-discontinuous style within a flat-lying, <4 km thick, top-to-the-north shear zone presently exposed along ~25 km of coastline (Nelson, 1982; Fagereng and Sibson, 2010; Fagereng, 2011). Initially, macroscopically ductile deformation mechanisms dominated and the sediments experienced compaction, volume loss and heterogeneous simple shear, developing a scaly cleavage and S/C-like shear structures (Nelson, 1982). During and after a time-progressive transition from ductile to brittle failure, a fault-fracture mesh filled by quartz-calcite veins developed, incorporating numerous anastomosing shear veins traceable for tens of meters (Fig. 3) (Nelson, 1982; Fagereng et al., 2010). This vein network is ubiquitous in mixed sandstone-mudstone outcrop throughout the shoreline exposures of the Chrystalls Beach Complex.

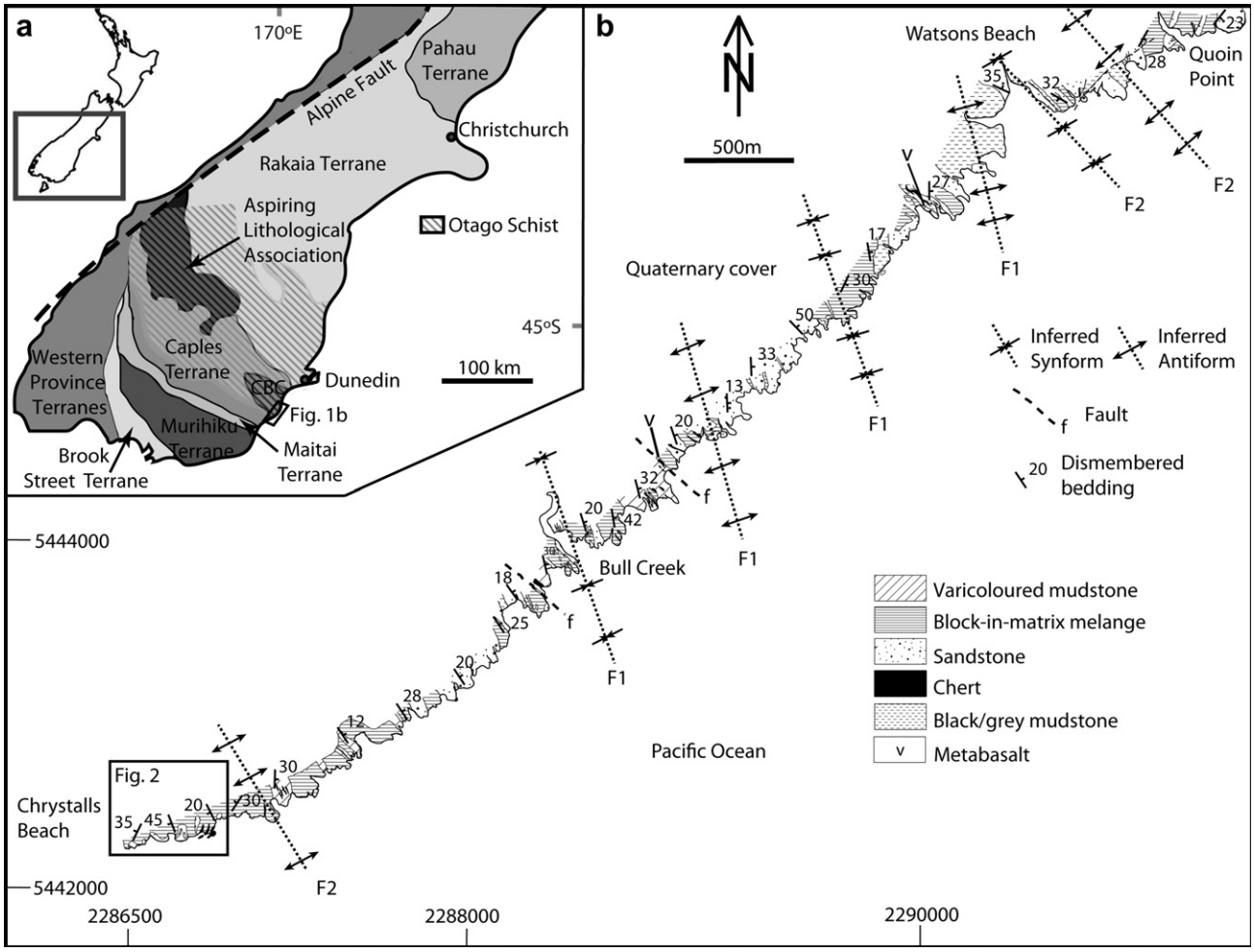

Fig. 1. a) Location of the Chrystalls Beach Complex and regional geological setting of the South Island of New Zealand. Geology after Bishop et al. (1985) and Mortimer (1993). b) Geology of coastal outcrops of the Chrystalls Beach Complex, after Nelson (1982), Hada et al. (1988), Hada et al. (2001), and Fagereng (2010). F1 are early, steeply inclined folds of dismembered bedding as inferred by Hada et al. (1988), F2 are open, upright folds of foliation and dismembered bedding.

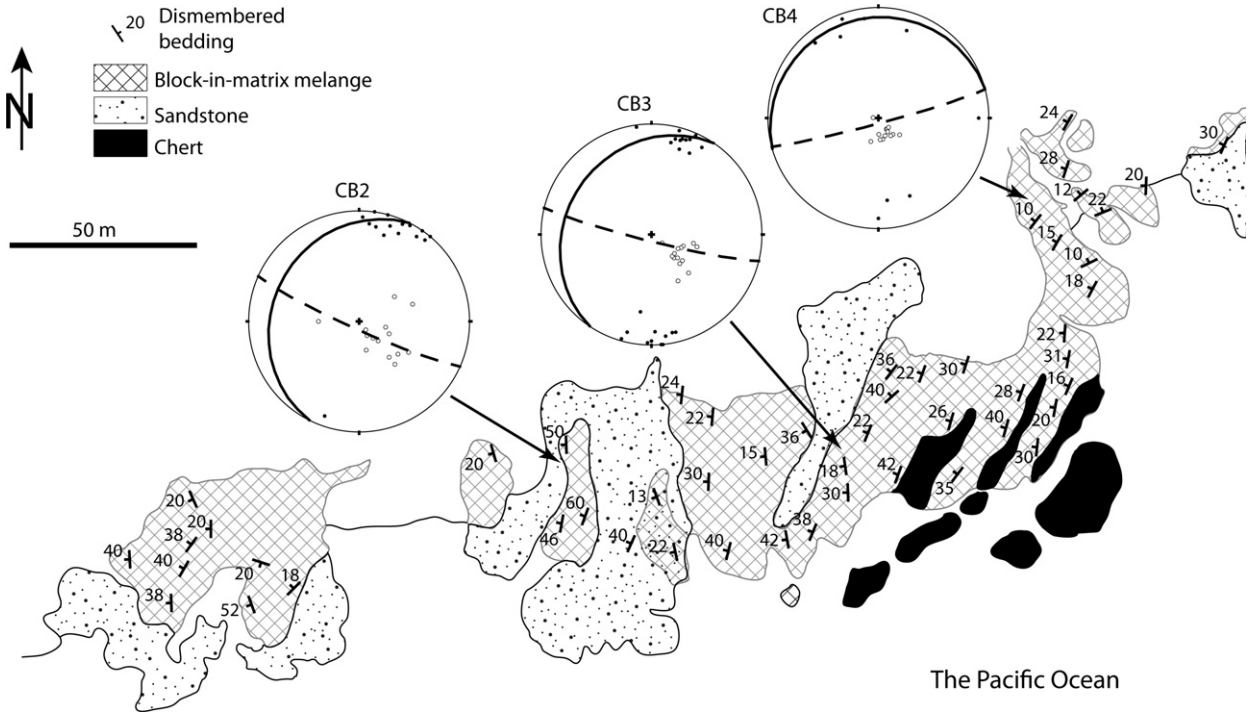

Fig. 2. Detailed geological map of the southernmost exposures of the Chrystalls Beach Complex. Equal-area stereoplots of poles to extension fractures (filled circles), and shear surfaces (open circles) for transect locations CB2, 3, and 4, where great circles show average orientations for shear (solid line) and extension fractures (dashed line).

2.2. Veins in the Chrystalls Beach Complex

The well developed network of anastomosing quartz-calcite veins includes mutually cross-cutting shallow-dipping slickenfibre-coated shear surfaces and subvertical extension veins (Figs. 2–4). Shear veins are divided into two sets: one comprises slickenfibre-coated surfaces subparallel to dismembered bedding and usually formed along a lithological contact, whereas a second set, comprising thinner veins, is observed subparallel to ductile S-planes (Fig. 4a). The vein fabrics generally show a top-to-the-north sense of shear, in agreement with asymmetry of the ductile fabric. However, variation in this shear sense is common, and a single fiber may show multiple directions of growth. Slickenfibre shear veins have multiple growth surfaces, a macroscopic crack-seal texture, and a pressure solution salvage is often visible along the vein margin (Fig. 4b).

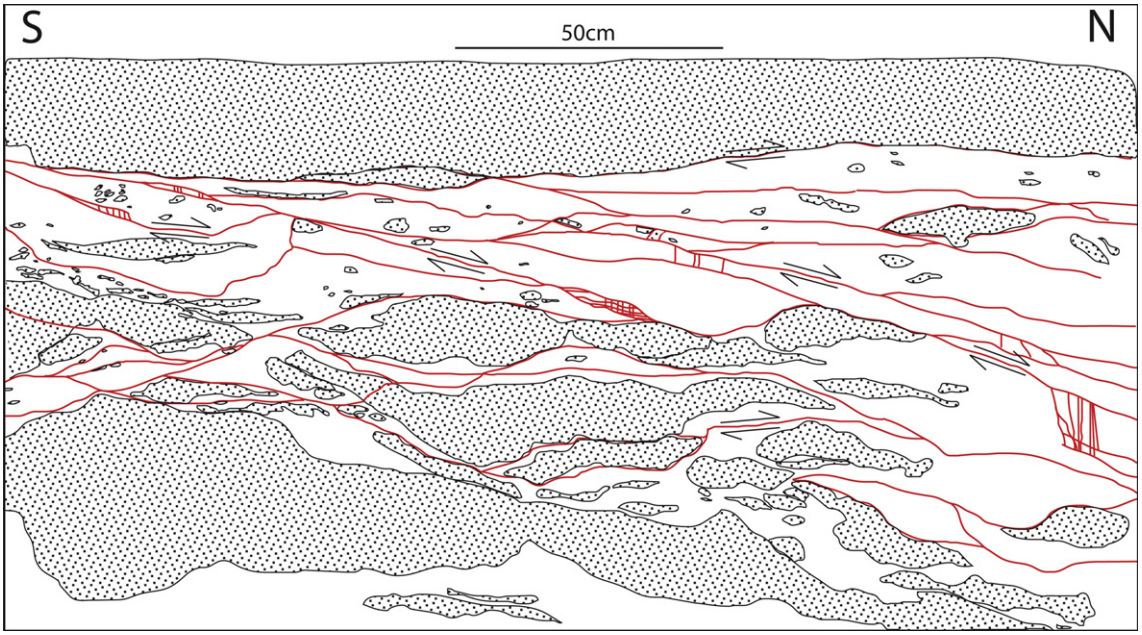

Fig. 3. Outcrop map of a vertical face in a typical Chrystalls Beach mélange outcrop. Gray = chert and sandstone, white = mudstone matrix, red lines = veins. (For interpretation of the references to colour in this figure legend, the reader is referred to the web version of this article.)

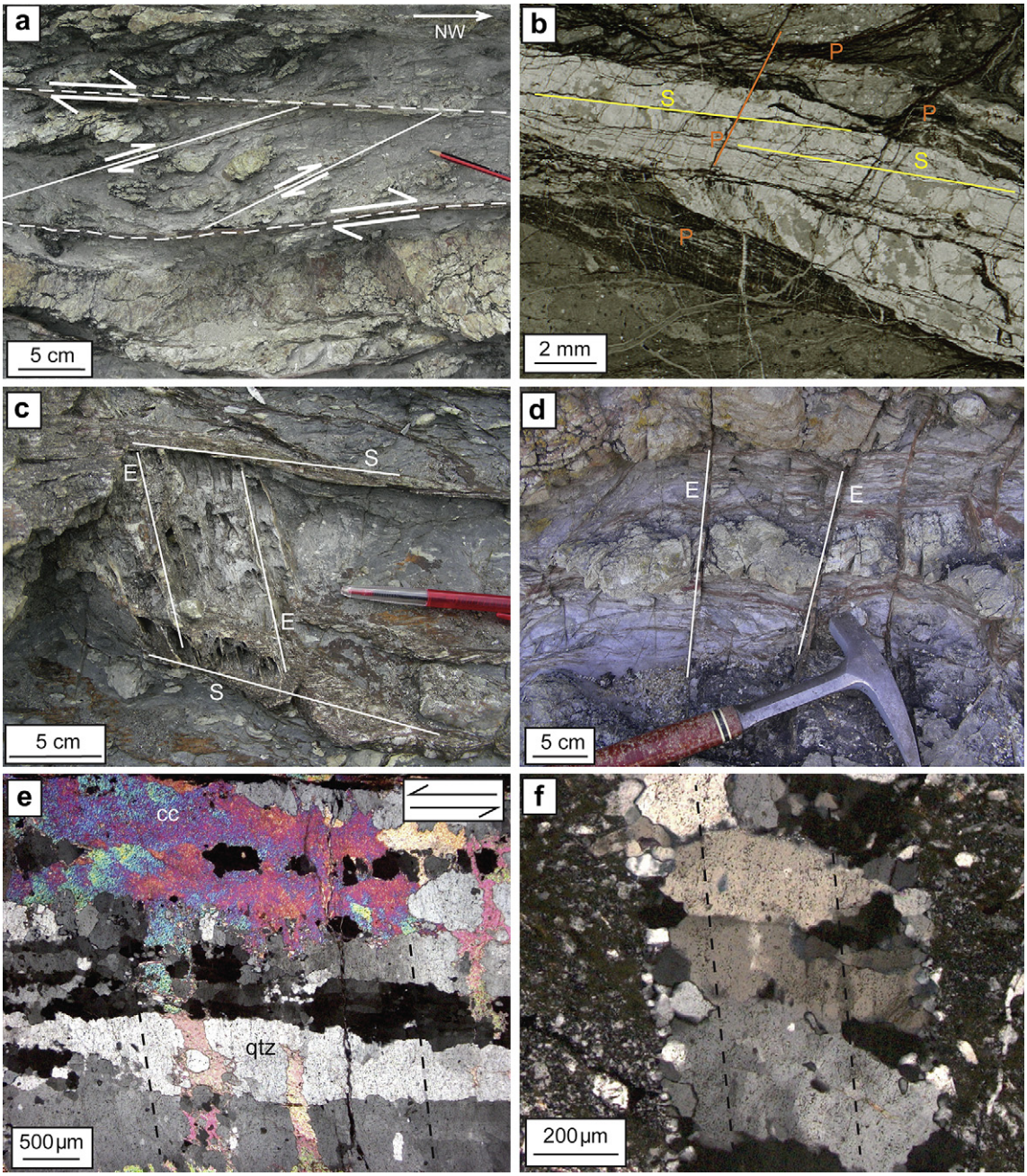

Fig. 4. a) General geometry of the Chrystalls Beach shear vein network: here two thicker shear veins (dashed white lines) subparallel to bedding are connected by thinner veins (solid white lines) subparallel to ductile S-planes as seen by rotated asymmetric lenses. Shear sense of top-to-the-north is evident. b) Photograph of thin section cut perpendicular to a shear vein. Note layered structure of vein indicating multiple slip surfaces (yellow, S) and the mutually cross-cutting relationship between the vein and pressure solution seams (orange, P). c) Dilational jog where two shear veins (S) are connected by numerous thin extension veins (E). d) Extension veins (E) are commonly at high angle to layering, and preferentially cut boudins where previously extended in the ductile regime. e) Photomicrograph of quartz (qtz) – calcite (cc) slickenfibres within a shear vein (crossed polars), note crack-seal structure with inclusion bands (dashed lines) near perpendicular to vein walls. f) Photomicrograph of vertical quartz extension vein (crossed polars). Note crack-seal structure with inclusion bands (dashed lines) developed parallel to vein walls. (For interpretation of the references to colour in this figure legend, the reader is referred to the web version of this article.)

Extension veins are typically subvertical and strike approximately perpendicular to slickenfibre trends (Fig. 2). Extension fractures are more common in competent layers. In particular, extension veins can be concentrated in dilational jogs (Fig. 4c), where they connect two adjacent shear veins. In addition, extension fractures are found preferentially at boudin necks, where boudins were not completely separated during ductile deformation and layer-parallel extension continued in a brittle mode (Fig. 4d).

Microscopically, both shear and extension veins show a 'crack-seal' structure (Fig. 4e,f). The spacing between inclusion trails is typically in the range of 10–50 μm, and appears to be roughly uniform along any particular crystal (Fagereng et al., 2010). In both kinematic vein types, elongate crystals track displacement magnitude and direction, perpendicular to vein walls in extension veins and at a small angle ($10^{\circ} \pm 5^{\circ}$) to the shear surface in slickenfibre shear veins (Fagereng et al., 2010).

3. Methodology

At outcrop scale, the vein system in the Chrystalls Beach Complex is sufficiently systematic to allow collection of representative vein distribution data in transects perpendicular to vein strike, as long as outcrops are chosen carefully (Fig. 2). This 1-d approach yields data that are comparable to many data sets in the literature, and also used because methods for analyzing 2-d and 3-d vein data are not as well developed (e.g. Gillespie et al., 1993, 1999; Pickering et al., 1995). For this study, vein thickness and spacing data were collected along linear transects in three exposures in the southern, lowest metamorphic grade, part of the Chrystalls Beach Complex (Fig. 2), chosen so that the distribution of both shear and extension veins within the assemblage could be analyzed. In addition, two transects were made through exposures by Watsons Beach, ~5 km further north in the complex (Fig. 1). Thickness was measured of veins ≥1 mm thick, thinner veins were recorded and their positions used to address vein spacing and clustering. Data for all transects are presented in Table 1, with a list of abbreviations in Table 2.

Extension and shear veins are treated as different vein sets for each transect (Table 1). The vein network in the Chrystalls Beach Complex is interpreted to have formed progressively in a relatively constant remote stress field (Nelson, 1982; Fagereng et al., 2010). Therefore, we assume that all extension veins can be grouped into one set, and similarly all shear veins are treated as one group.

Table 2
List of symbols and abbreviations used in this study.

Symbol	Meaning
D_t	Fractal dimension of thickness distribution
t	Vein thickness
$N(r)$	Number of objects size r or greater
s	Vein spacing
D_c	Fractal dimension of vein clustering
C_v	Coefficient of variance
ΔL	Bulk extensional strain
L_f	Final length
L_i	Initial length
V_f	Total thickness of veins along a transect

4. Results

4.1. Vein thickness distribution

Vein thickness distributions have previously been reported as power-law (e.g. Clark et al., 1995; Johnston and McCaffery, 1996; Gillespie et al., 1999; André-Mayer and Sausse, 2007; Sanderson et al., 2008) and log-linear (e.g. Narr and Suppe, 1991; McCaffrey et al., 1993; Foxford et al., 2000). Power-law distributions follow the proportionality

$$N(r) \propto r^{-D} \quad (1)$$

where $N(r)$ is the number of objects of size r or larger. This distribution is fractal, and D represents the fractal dimension (Mandelbrot, 1982). In a frequency-size distribution of vein thickness, t, the value of the fractal dimension, D_t, theoretically depends on the difference in nucleation and growth rate (Clark et al., 1995). The end-member vein thickness populations are therefore (Clark et al., 1995): (1) a scenario where all fracture events are nucleation events, all veins are the same thickness, and $D_t = \infty$, and (2) a situation where all events are growth events and $D_t = 0$. D_t also represents the difference in growth on thin and thick veins, where $D_t > 1$ indicates that thinner veins accommodate a significant proportion of total extension (Scholz and Cowie, 1990; Clark et al., 1995; Fisher et al., 1995; Sanderson et al., 2008). Therefore, D_t also represents a measure of localization, as smaller values of D_t indicate a greater proportion of thick veins, and thus localization of deformation on these features rather than formation of new, thin, fractures (e.g. Sanderson et al., 1994, 2008; Sanderson and Zhang, 2004).

In the Chrystalls Beach Complex, the analyzed outcrops show a power-law thickness distribution (Table 1, Figs. 5–7). The fit to a power-law distribution is very good, likely because only veins with thickness ≥1 mm were considered, and therefore roll-off effects at small thicknesses are not observed – contrary to other studies of power-law distributions over larger range in t (c.f. Pickering et al., 1995). D_t is between 1 and 2, but is >3 in one outcrop (Table 1). When plotting all shear and extension veins, two power-law distributions with slightly different D_t values are obtained (Fig. 5). For shear veins, $D_t = 1.69$, while for extension veins, $D_t = 1.85$. As the sample sets are relatively small, the difference between these fractal dimensions is too small to indicate a statistical difference between shear and extension vein thickness distributions.

The calculated values for D_t assume no deformation after vein formation. Although the vein system studied is amongst the latest deformation in the Chrystalls Beach Complex (Fagereng et al., 2010), the shear veins are commonly affected by pressure solution subparallel to the vein walls (Fig. 4b), and the vein thicknesses may therefore be reduced by dissolution (c.f. Ortega et al., 2010). However, dissolution by pressure solution would tend to preferentially reduce the thickness of thinner veins, leading to a thickness distribution with underestimated D_t. Thus, the high D_t in the Chrystalls Beach Complex is unlikely to be an artifact of pressure solution effects, and if anything is an underestimated value.

Table 1
Transect properties, showing length of transect, number of veins intersected, vein intensity, and rock type (S = sandstone, M = mélange, MM = mudstone). This is followed by statistical data; V_t is the total vein thickness intersected, while ΔL refers to % inferred increase in length by vein growth. D_t and D_c are the fractal dimensions of thickness and clustering respectively, and R^2 refers to the coefficients of determination for the regression performed to arrive at these D values. C_v is the coefficient of variance for vein spacing.

Transect	Length (cm)	# of veins	Vein intensity (m^{-1})	Rock	V_t (mm)	ΔL (%)	D_t	R^2	D_c	R^2	C_v
Extension veins											
CB2e	370	128	35	S	149	4.2	3.01	0.999	0.78	0.996	1.17
CB3e	519	139	27	S	257	5.2	1.59	0.979	0.65	0.990	3.00
Shear veins											
CB2s	76	38	50	M	49	6.9	2.07	0.957	0.66	0.997	1.46
CB3s1	393	77	20	M	162	4.3	1.40	0.954	0.47	0.981	1.20
CB3s2	110	39	36	M	65	6.3	1.54	0.985	0.60	0.996	1.49
CB4s1	54	33	61	M	60	12.5	1.59	0.983	0.70	0.984	1.07
CB4s2	57	60	105	M	98	20.8	1.24	0.886	0.81	0.992	0.82
WB2	230	112	49	M + MM	176	8.3	1.44	0.953	0.78	0.998	1.11
WB4	137	103	75	MM	156	12.9	1.80	0.959	0.85	0.999	1.06

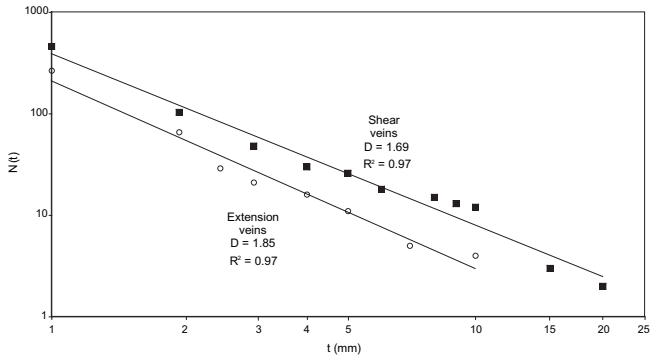

Fig. 5. Plot of log t versus log $N(t)$ where t is vein thickness and $N(t)$ is the number of veins of thickness t or greater. Filled squares represent shear veins and open circles represent extension veins. D is fractal dimension and R^2 is the coefficient of determination.

4.2. Vein spacing distribution

Vein spacing is also analyzed comparing r and $N(r)$ as defined in Eq. (1). Defining s as the spacing between veins, plots of $N(s)$ versus s should define a straight line in log–log space for a power-law frequency-size distribution. An example from outcrop CB3e is shown in Fig. 6, where the frequency-size distribution diverges from power-law at small vein spacing. A similar effect is seen when plotting $N(s)$ against s for all shear and extension veins (Fig. 8). The shape of the spacing distributions for shear and extension veins are both convex-up on log–log axes and convex-down on log-linear axes.

Vein spacing distribution is clearly not linear (Fig. 8a), but could be interpreted as either log-linear (Fig. 8b) or power-law (Fig. 8c). However, accounting for roll-off effects at small vein spacing (Pickering et al., 1995; Blenkinsop and Sanderson, 1999), and underrepresentation of large vein spacing in a limited data set, the

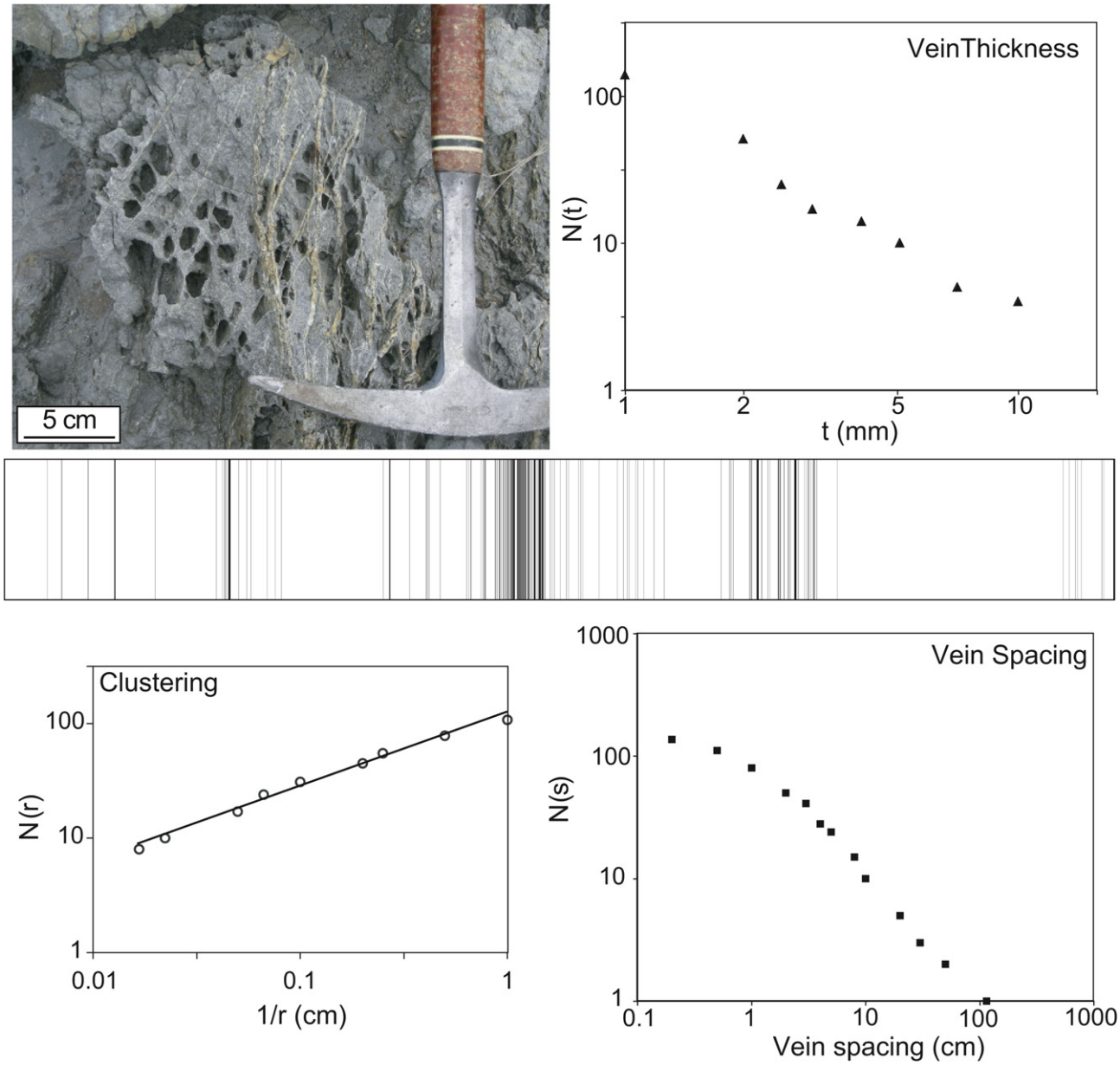

Fig. 6. Left to right: Photo of typical vein cluster intersecting transect CB3e, thickness distribution, vein log, clustering and vein spacing distributions for transect CB3e, through extension veins in a large sandstone unit.

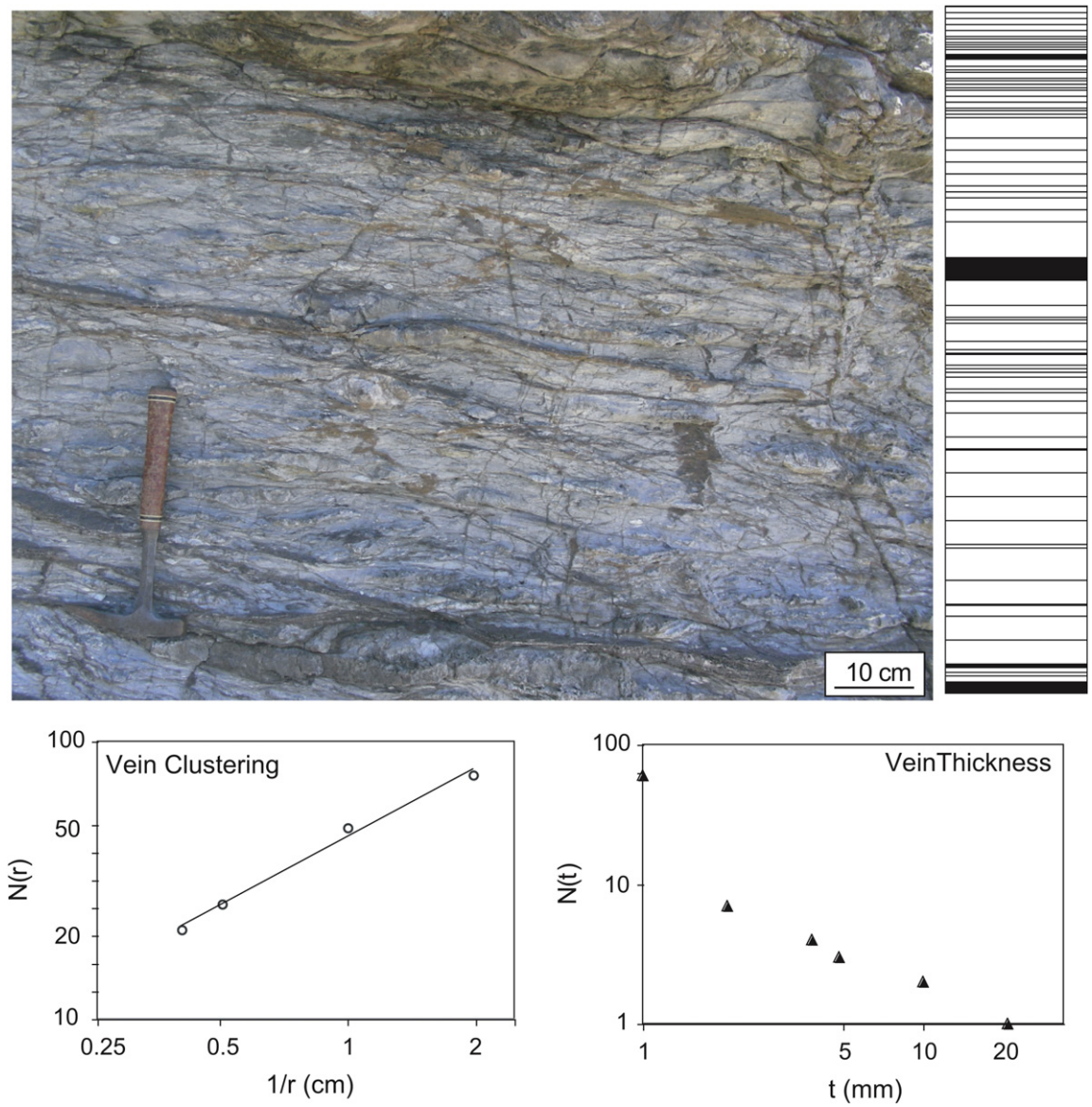

Fig. 7. From left to right: Outcrop photograph, vein log, and clustering and thickness for transect CB4s2, dominated by subhorizontal shear veins in a mélange with low proportion of competent lenses. Note very high vein intensity (>100 fractures/m) in this outcrop.

fit to a power-law distribution is better than the log–linear fit (Fig. 8). Thus, the vein spacing in the Chrystalls Beach Complex appears to follow a fractal distribution within the sampled range of spacing (fractal range approximately 0.5–20 cm). Note that this range is small, and the spatial distribution of fractures may be different at length scales above and below this fractal range (Ortega et al., 2006).

4.3. Box-counting of vein clustering

As vein spacing is not uniform, a degree of clustering should be expected. Manning (1994) proposed a box-counting technique for measuring clustering of metamorphic veins. This method uses linear vein transects where the position of intersections between veins and the transect are mapped. The map is then divided into segments of length r, and the number of segments $N(r)$ containing at least one vein are counted. If a vein set is fractal, it has a constant fractal dimension $0 \leq D_c \leq 1$ (Mandelbrot, 1982; Turcotte, 1997) such that (Manning, 1994)

$$D_c = \partial(\log N(r))/\partial(\log 1/r) \quad (2)$$

If D_c is constant, then the vein set is fractal and scale invariant for the considered range in r (typically 1 mm to ~0.5 m in the current study). D_c is a measure of 'space-filling', i.e. $D_c = 0$ if no veins are intersected and $D_c = 1$ if the transect is completely filled by veins. It follows that D_c is large for a pervasive, anticlustered vein network, and small for a highly clustered vein system (Manning, 1994).

As in vein thickness distributions, the data are similar for all transects (Table 1, Figs. 6 and 7). The values of D_c vary from 0.40 to 0.85, i.e. indicating moderate degrees of clustering. The smallest values are observed in mélange outcrops, while the largest values are measured in relatively homogeneous mudstone and sandstone. The one mélange with a large D_c (CB4s2, =0.81) has a relatively small sand/mud ratio and very strong vein intensity (Fig. 7).

The coefficient of variance, C_v, provides a second measure of clustering and is the ratio of the standard deviation and the mean. Gillespie et al. (1999) demonstrated that $C_v > 1$ if veins are

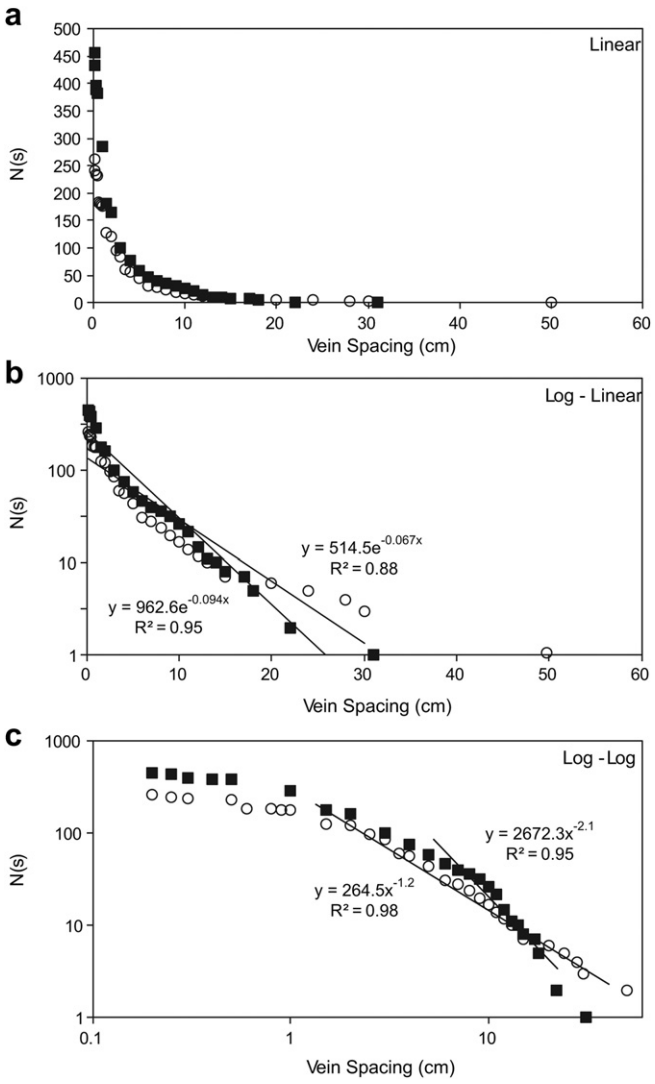

Fig. 8. Number of measurements $N(s)$ greater than a spacing s, plotted against s, for extension veins (open circles) and shear veins (filled squares) on linear, log–linear and log–log axes. Best fit equations and coefficients of determination (R^2) shown for regression performed on log–linear and log–log plots.

clustered, $C_v = 1$ for random vein distribution and $C_v < 1$ for pervasive, anticlustered vein systems. $1.0 < C_v < 1.5$ for 7 of the 9 transects in the Chrystalls Beach Complex, indicating random to moderately clustered vein systems (Table 1). The only transect where $C_v < 1$ is CB4s2, where a large D_c also indicates a pervasive fracture system. In CB3e, C_v is 3.0, indicating high degree of clustering. However, while C_v and D_c are generally weakly correlated with large D_c corresponding to small C_v, the very large C_v in CB3e is not correlated to a particularly small D_c. The weak correlation between C_v and D_c is likely an effect of the small considered range in spacing values and consequent large uncertainties in the statistical parameters.

4.4. Bulk extensional strain

Bulk extensional strain was calculated along each transect, as a measure of dilation perpendicular to the vein walls. The % bulk extensional strain parallel to the orientation of the transect is

$$\Delta L = 100\left[\left(L_f - L_i\right)/L_i\right] = 100\left[V_t/\left(L_f - V_t\right)\right] \quad (3)$$

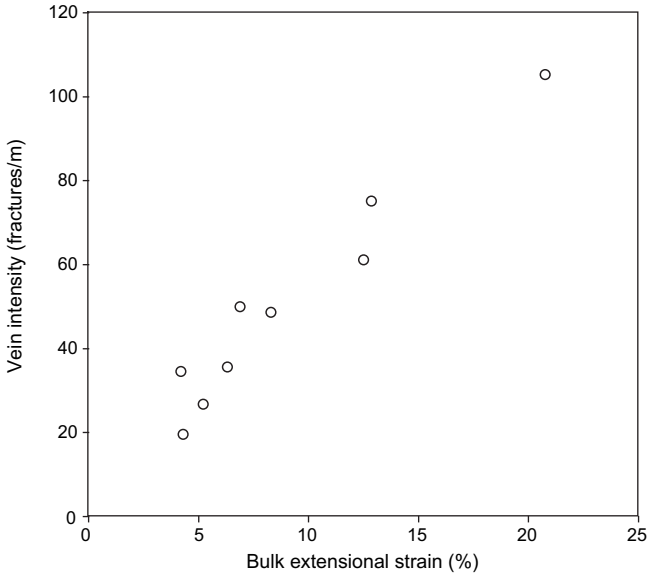

Fig. 9. Plot of bulk extensional strain ($\Delta L = 100[(L_f - L_i)/L_i]$) along each transect against vein intensity. Note the strong linear correlation with high bulk extensional strain relating to high vein intensity.

where L_f and L_i are the final and initial lengths of the segment and V_t is the total thickness of veins intersected by the transect (Foxford et al., 2000). L_f is the length of the transect, and L_i is the length of the transect minus V_f. For extension veins, the extensional strain equals the dilation achieved by vein opening. For shear veins, the extensional strain represents dilation perpendicular to the shear surface, and is not equal to the total extension accommodated by shear vein growth.

The greatest extensional strains, $\Delta L > 10\%$, are measured in vertical transects through shear veins in mélange or mudstone. This relationship suggests that much dilatancy is associated with shear displacement in the mélange. A positive correlation exists between vein intensity (fractures per meter transect) and ΔL (Fig. 9), indicating that large ΔL relates to outcrops that experienced pervasive, distributed fracturing, forming many veins in a given area.

4.5. Summary of observations

The thickness distribution of the Chrystalls Beach Complex fault-fracture mesh is fractal and self-similar, with relatively large fractal dimensions indicating that thin veins accommodated much of the dilation. The thickness distribution is similar for extension and shear veins. Veins have a power-law spacing distribution, and range from randomly distributed to moderately clustered within the considered exposures.

5. Discussion

Models by Clark et al. (1995) predicted that, for extension veins, a power-law thickness distribution is reproduced by growth rates proportional to thickness. A power-law thickness distribution may therefore be produced when relatively thick veins stay partly open longer than thinner veins (Clark et al., 1995). This effect should be seen microstructurally by larger inclusion band spacing for younger bands (Clark et al., 1995; Fisher et al., 1995). Both shear and extension veins in the Chrystalls Beach Complex, however, have nearly constant crack-seal spacing. Thick extension veins therefore reflect a greater number of opening events, and a characteristic aperture for these events. Shear veins, however, open at a very

small angle to the vein walls, and therefore their thickness is not determined by the duration they stay partly open, but rather the number of internal slip surfaces (Fagereng et al., 2010). Shear may occur preferentially on weak planes, such as pre-existing fractures or cleavage planes, or within zones of localized deformation governed by the distribution of mechanical heterogeneities (Fagereng and Sibson, 2010; Fagereng, 2011). Thick shear veins are therefore interpreted to occur by repeated shear fracturing in zones of concentrated deformation. Thin shear veins, however, occur within areas of distributed deformation or where shear is not accompanied by dilation.

Vein distributions in heterogeneous rock assemblages such as the Chrystalls Beach Complex are interpreted to be affected by mechanical variation between rock types. Gillespie et al. (1999) compared stratabound and non-stratabound veins. They found that thickness and spacing distributions of stratabound veins are commonly non-power-law and follow a characteristic length-scale determined by lithological layering. Non-stratabound veins, on the other hand, have a power-law thickness distribution ($0.5 < D_t < 1.2$), but a clustered ($C_v > 1$), log–linear spacing distribution (Gillespie et al., 1999). Chrystalls Beach veins have a high D_t, indicating a large proportion of thin veins, and a weakly clustered ($C_v > 1$), power-law distribution in space. Vein distributions within the fault-fracture mesh are therefore not compatible with a length-scale controlled by lithological layering. Instead, distributed shear and extension within the fracture network created a power-law vein thickness distribution characterized by a large fractal dimension suggesting minor localization (c.f. Sanderson et al., 2008). This vein thickness distribution is comparable to the extension vein system in the Kodiak Complex – another subduction-related vein network – which has a power-law thickness distribution with $D_t = 1.33$ (Clark et al., 1995; Fisher et al., 1995). Weak to moderate clustering in some outcrops could be caused by preferential fracturing of rock with greater tensile strengths (e.g. Fig. 4d) or stress risers at the boundaries of competent phacoids (Fig. 4a) (Fagereng, 2011).

Formation of a dense, anastomosing network of predominantly thin veins is also described by Holland and Urai (2010). They inferred that deformation was not localized to a single fracture, but rather yielded a fracture network during an event where fractures were sealed by strong cement of hydrothermal precipitates. Because both shear and extension veins in the Chrystalls Beach Complex are cemented by quartz-calcite mineralization, which is likely stronger than the surrounding, cleaved, phyllosilicate-dominated matrix, preferential deformation of weaker matrix is inferred to result in the formation of new fractures rather than preferential growth of a few larger veins. Thus, the thickness distribution indicating predominance of thin veins implies that, as proposed by Holland and Urai (2010), anastomosing vein systems form where vein fills are stronger than wall rock.

The shear veins in the Chrystalls Beach Complex are interpreted to form at high angles to the greatest principal compressive stress by shear along pre-existing weak cleavage planes (Fagereng et al., 2010). If new shear veins form along weak planes in the wall rock, in preference to reactivation of existing veins, one would expect clusters of thin veins to occur instead of a few thick veins. Thus, the weak clustering apparent in some exposures is representative of clusters of thin veins having formed in locations of increased localized deformation. The reason for such localization of shear veins is related to mechanical anisotropy within the mélange (Fagereng and Sibson, 2010; Fagereng, 2011). In clustered extension vein populations, which are generally constrained to relatively homogeneous sandstone (e.g. Fig. 6), heterogeneous fluid pressure distribution (Foxford et al., 2000) or subcritical crack growth (Olson, 1993, 2004) may also have caused weak clustering. As opposed to many economically mineralized vein systems, which are commonly characterized by power-law vein thickness distributions with low D_t (<1) and focused fluid flow though a connected system of few thick veins (Sanderson et al., 1994, 2008; Roberts et al., 1999), the mélange vein network appears pervasive and dominated by many thin veins. Thus, the fault-fracture mesh represents distributed fracturing, and likely allowed for pervasive rather than localized fluid flow, within a mélange. It is characterized by a weakly clustered, power-law vein distribution with a large fractal dimension. This conclusion is supported by a good correlation between vein intensity and bulk extensional strain (Fig. 9), which also suggests that strain was accommodated by high fracture intensity as opposed to continued reopening of few thick veins.

6. Conclusions

The vein system of the Chrystalls Beach Complex is characterized by a power-law thickness distribution with a large fractal dimension. Spacing is inferred to be power-law, but the inference is limited because the data set is small and over a limited fractal length-scale.

The greatest D_t values are recorded in transects through extension veins in relatively homogeneous sandstone, where veins are essentially non-stratabound. Within these more competent rocks, pervasive failure was probably dominated by distributed hydraulic extension fracture of intact, relatively high tensile strength rock. Weak clustering results from variations in fluid pressure (e.g. Foxford et al., 2000), or increased tensile stress around the crack-tip of subcritical fractures (Olson, 1993, 2004).

Shear veins generally also have thickness distributions with large D_t indicating distributed deformation, although some transects show large C_v and small D_c indicating weak clustering. The clusters of thin veins, and the few thick veins, represent zones of localized and concentrated brittle deformation. Clusters of thin veins likely formed rather than single, thick veins as quartz-calcite cemented fractures were stronger than the cleaved mudstone matrix (c.f. Holland and Urai, 2010). $D_t > 1$ for the shear vein population therefore suggests that distributed brittle deformation accommodated much of the displacement in the mélange, by slip on numerous discontinuities within a ductilely flowing matrix. A positive correlation between bulk extensional strain and vein intensity (Fig. 9) supports the conclusion that distributed shear on many thin veins was an important mechanism in the complex. The mélange deformed predominantly by distributed, high intensity, shear and extension fracture.

Acknowledgments

This paper arises from a Ph.D. thesis supervised by R.H. Sibson, whose constructive criticism was invaluable for the study. The work was funded by a GNS Science Hazards Scholarship. Thorough reviews by O. Ortega and D.J. Sanderson, and the editorial assistance of W. Dunne, significantly improved the manuscript.

References

André-Mayer, A.-S., Sausse, J., 2007. Thickness and spatial distribution of veins in a porphyry copper deposit, Rosia Poieni, Romania. Journal of Structural Geology 29, 1695–1708.

Barker, S.L.L., Cox, S.F., Eggins, S.M., Gagan, M.K., 2006. Microchemical evidence for episodic growth of antitaxial veins during fracture-controlled fluid flow. Earth and Planetary Science Letters 250, 331–344.

Bishop, D.G., Bradshaw, J.D., Landis, C.A., 1985. Provisional terrane map of south Island, New Zealand. In: Howell, D. (Ed.), Tectonostratigraphic Terranes. Circumpacific Council for Energy and Mineral Resources, pp. 515–521. vol. 1 of Earth Science Series.

Blenkinsop, T.G., Sanderson, D.J., 1999. Are gold deposits in the crust fractals? A study of gold mines in the Zimbabwe craton. In: McCaffrey, K.J.W., Lonergan, L., Wilkinson, J.J. (Eds.), Fractures, Fluid Flow and Mineralization.

Geological Society of London Special Publication. Geological Society of London, vol. 155, pp. 141–151.
Clark, M.B., Brantley, S.L., Fisher, D., 1995. Power-law vein-thickness distributions and positive feedback in vein growth. Geology 23, 975–978.
Coombs, D.S., Landis, C.A., Hada, S., Ito, M., Roser, B.P., Suzuki, T., Yoshikura, S., 2000. Geochemistry and terrane correlation of the Chrystalls Beach-Brighton coastal block, southeast Otago, New Zealand. New Zealand Journal of Geology and Geophysics 43, 355–372.
Cox, S.F., Etheridge, M.A., 1983. Crack-seal fibre growth mechanisms and their significance in the development of oriented layer silicate microstructures. Tectonophysics 92, 147–170.
Fagereng, Å., 2010. Subduction-related Fault Processes – Ancient and Active. In: Ph.D. Thesis, University of Otago. Dunedin, Newzealand, 521 pp.
Fagereng, Å., 2011. Frequency-size distribution of competent lenses in a block-in-matrix mélange: imposed length scales of brittle deformation? Journal of Geophysical Research, doi:10.1029/2010JB007775.
Fagereng, Å, Cooper, A.F., 2010a. Petrology of metabasalts from the Chrystalls Beach accretionary mélange – implications for tectonic setting and terrane origin. New Zealand Journal of Geology and Geophysics 53, 57–70.
Fagereng, Å, Cooper, A.F., 2010b. The metamorphic history of rocks buried, accreted and exhumed in an accretionary prism: an example from the Otago Schist, New Zealand. Journal of Metamorphic Geology 28, 935–954.
Fagereng, Å, Remitti, F., Sibson, R.H., 2010. Shear veins observed along planar anisotropy at high angles to greatest compressive stress. Nature Geoscience 3, 482–485. doi:10.1038/NGEO898.
Fagereng, Å, Sibson, R.H., 2010. Mélange rheology and seismic style. Geology 38, 751–754. doi:10.1130/G30868.1.
Fisher, D., Brantley, S.L., Everett, M., Dzvonik, J., 1995. Cyclic fluid flow through a regionally extensive fracture network within the Kodiak accretionary prism. Journal of Geophysical Research 100 (B7), 12,881–12,894.
Foxford, K.A., Nicholson, R., Polya, D.A., Hebblethwaite, R.P.B., 2000. Extensional failure and hydraulic valving at Minas da Panasqueira, Portugal: evidence from vein spacial distributions, displacements and geometries. Journal of Structural Geology 22, 1065–1086.
Gillespie, P.A., Howard, C., Walsh, J.J., Watterson, J., 1993. Measurement and characterisation of spatial distribution of fractures. Tectonophysics 226, 113–141.
Gillespie, P.A., Johnston, J.D., Loriga, M.A., McCaffrey, K.J.W., Walsh, J.J., Watterson, J., 1999. Influence of layering on vein systematics in line samples. In: McCaffrey, K.J.W., Lonergan, L., Wilkinson, J.J. (Eds.), Fractures, Fluid Flow and Mineralization. Geological Society of London Special Publication. Geological Society of London, vol. 155, pp. 35–56.
Hada, S., Yoshikura, S., Aita, Y., Sato, K., 1988. Notes on the geology and paleontology of the Chrystalls Beach Complex, south Island, New Zealand. In: Preliminary Report on the Accretion Complex Geology of Otago Coast Section in the South Island, New Zealand. Department of Geology, Faculty of Science, Kochi University, Japan, pp. 21–28.
Hada, S., Ito, M., Landis, C.A., Cawood, P., 2001. Large-scale translation of accreted terranes along continental margins. Gondwana Research 4, 628–629.
Hill, D.P., 1977. A model for earthquake swarms. Journal of Geophysical Research 82, 1347–1352.
Holland, M., Urai, J.L., 2010. Evolution of anastomosing crack-seal vein networks in limestones: insight from an exhumed high-pressure cell, Jabal Shams, Oman Mountains. Journal of Structural Geology 32, 1279–1290.
Johnston, J.D., McCaffrey, J.W., 1996. Fractal geometry of vein systems and the variation of scaling relationships with mechanism. Journal of Structural Geology 18, 349–358.
Mandelbrot, B.B., 1982. The Fractal Geometry of Nature. W.H. Freeman, San Francisco.
Manning, C., 1994. Fractal clustering of metamorphic veins. Geology 22, 335–338.
McCaffrey, K., Johnson, J.D., Feely, M., 1993. Use of fractal statistics in the analysis of Mo–Cu mineralization at Mace Head, County Galway. Irish Journal of Earth Sciences 12, 139–148.
Mortimer, N., 1993. Geology of the Otago Schist and Adjacent Rocks. Scale 1:500 000. Institute of Geological and Nuclear Sciences geological map 7, GNS Science, Lower Hutt, New Zealand.
Mortimer, N., 2000. Metamorphic discontinuities in orogenic belts: example of the garnet–biotite–albite zone in the Otago Schist, New Zealand. International Journal of Earth Sciences 89, 295–306.
Mortimer, N., 2003. A provisional structural thickness map of the Otago Schist, New Zealand. American Journal of Science 303, 603–621.
Narr, W., Suppe, J., 1991. Joint spacing in sedimentary rocks. Journal of Structural Geology 13, 1037–1048.
Nelson, K.D., 1982. A suggestion for the origin of mesoscopic fabric in accretionary melange, based on features observed in the Chrystalls Beach Complex, South Island, New Zealand. Geological Society of America Bulletin 93, 625–634.
Olson, J.E., 1993. Joint pattern development: effects of subcritical crack growth and mechanical crack interaction. Journal of Geophysical Research 98, 12,251–12,265. doi:10.1029/93JB00779.
Olson, J.E., 2004. Predicting fracture swarms – the influence of subcritical crack growth and the crack-tip process zone on joint spacing in rock. In: Cosgrove, J.W., Engelder, T. (Eds.), The Initiation, Propagation, and Arrest of Joints and Other Fractures. Geological Society of London Special Publication. Geological Society of London, vol. 231, pp. 73–87.
Ortega, O.J., Marrett, R.A., Laubach, S.E., 2006. A scale-independent approach to fracture intensity and average spacing measurement. American Association of Petroleum Geologists Bulletin 90, 193–208.
Ortega, O.J., Gale, J.F.W., Marrett, R., 2010. Quantifying diagenetic and stratigraphic controls on fracture intensity in platform carbonates: an example from the Sierra Madre Oriental, northeast Mexico. Journal of Structural Geology 32, 1943–1959.
Passchier, C.W., Trouw, R.A.J., 2005. Microtectonics, second ed. Springer-Verlag, Berlin.
Pickering, G., Bull, J.M., Sanderson, D.J., 1995. Sampling power-law distributions. Tectonophysics 248, 1–20.
Ramsay, J.G., 1980. The crack–seal mechanism of rock deformation. Nature 284, 135–139.
Ramsay, J.G., Huber, M.I., 1987. Folds and Fractures. The Techniques of Modern Structural Geology, vol. 2. Academic Press, London.
Robert, F., Boullier, A.-M., Firdaous, K., 1995. Gold–quartz veins in metamorphic terranes and their bearing on the role of fluids in faulting. Journal of Geophysical Research 100, 12,861–12,879.
Roberts, S., Sanderson, D.J., Gumiel, P., 1999. Fractures, Fluid Flow and Mineralization. In: Special Publications. Geological Society of London, vol. 155, Ch. Fractal Analysis and Percolation Properties of Veins, pp. 7–16.
Sanderson, D.J., Zhang, X., 2004. Stress Controlled Localisation of Deformation and Fluid Flow in Fractured Rocks. In: Special Publication of the Geological Society of London, vol. 231, pp. 299–314.
Sanderson, D.J., Roberts, S., Gumiel, P., 1994. A fractal relationship between vein thickness and gold grade in drill core from La Codosera, Spain. Economic Geology 89, 168–173.
Sanderson, D.J., Roberts, S., Gumiel, P., Greenfield, C., 2008. Quantitative analysis of tin and tungsten bearing sheeted vein systems. Economic Geology 103, 1043–1056.
Scholz, C.H., Cowie, P.A., 1990. Determination of total strain from faulting using slip measurements. Nature 350, 838–840.
Sibson, R.H., 1987. Earthquake rupturing as a mineralizing agent in hydrothermal systems. Geology 15, 701–704.
Sibson, R.H., 1996. Structural permeability of fluid-driven fault-fracture meshes. Journal of Structural Geology 18, 1031–1043.
Simpson, G.D.H., 2000. Synmetamorphic vein spacing distributions: characterisation and origin of a distribution of veins from NW Sardinia, Italy. Journal of Structural Geology 22, 335–348.
Turcotte, D.L., 1997. Fractals and Chaos in Geology and Geophysics, second ed. Cambridge University Press, Cambridge, UK.
Urai, J.L., Williams, P.F., van Roermund, H.L.M., 1991. Kinematics of crystal growth in syntectonic fibrous veins. Journal of Structural Geology 13, 823–836.
Velde, B., Dubois, J., Moore, D., Touchard, G., 1991. Fractal patterns of fractures in granites. Earth and Planetary Science Letters 104, 23–35.